

Scaling Distributed Training with Adaptive Summation

Saeed Maleki, Madan Musuvathi, Todd Mytkowicz, Olli Saarikivi
Microsoft Research

Tianju Xu, Vadim Eksarevskiy, Jaliya Ekanayake, Emad Barsoum
Microsoft

{saemal, madanm, toddm, olsaarik, tix, vaeksare, jaliyaek, ebarsoum}@microsoft.com

Abstract

Stochastic gradient descent (SGD) is an inherently sequential training algorithm—computing the gradient at batch i depends on the model parameters learned from batch $i - 1$. Prior approaches that break this dependence do not honor them (e.g., sum the gradients for each batch, which is not what sequential SGD would do) and thus potentially suffer from poor convergence. This paper introduces a novel method to combine gradients called Adasum (for adaptive sum) that converges faster than prior work. Adasum is easy to implement, almost as efficient as simply summing gradients, and is integrated into the open-source toolkit Horovod.

This paper first provides a formal justification for Adasum and then empirically demonstrates Adasum is more accurate than prior gradient accumulation methods. It then introduces a series of case-studies to show Adasum works with multiple frameworks, (TensorFlow and PyTorch), scales multiple optimizers (Momentum-SGD, Adam, and LAMB) to larger batch-sizes while still giving good downstream accuracy. Finally, it proves that Adasum converges.

To summarize, Adasum scales Momentum-SGD on the MLPerf Resnet50 benchmark to 64K examples before communication (no MLPerf entry converged with more than 16K), the Adam optimizer to 64K examples before communication on BERT-LARGE (prior work showed Adam stopped scaling at 16K), and the LAMB optimizer to 128K before communication on BERT-LARGE (prior work used 64K), all while maintaining downstream accuracy metrics. Finally, if a user does not need to scale, we show LAMB with Adasum on BERT-LARGE converges in 30% fewer steps than the baseline.

1 Introduction

Recent trends in deep learning demonstrate that increasing model size, coupled with an increase in training data, results in improved model performance. This has led to progressively larger models, such as BERT [14], GPT-2 [27], Megatron [34],

and UniLM [15]. This trend along with the end of Moore’s law means that these large models require massively parallel architectures to train. An important source of parallelism in training is data parallelism where individual nodes train on a subset of data and periodically exchange model updates. Unfortunately, this is at odds with the sequential nature of stochastic gradient descent (SGD) which is the most common algorithm to train them. Some prior approaches break this sequential dependence with asynchronous SGD [13, 30] where individual nodes asynchronously update a global model ignoring potential staleness of model updates. Recent advances in hardware with powerful compute nodes with fast interconnects [1, 8, 9] have led to synchronous SGD where one trains with very large minibatch sizes. Neither approach is a panacea as both staleness and naively increasing minibatch sizes reduces model convergence [17, 20, 21]

This paper proposes a new approach to data parallelism based on two key insights. First, rather than asynchronously updating a global model or increasing the minibatch size, this approach attempts to *emulate* a sequential execution in parallel. The basic idea is to combine the individual model updates from nodes, each obtained by running a (small) minibatch from a starting model, into an update that would have resulted had these nodes run one after the other from the same starting model. Second, this sequential emulation allows us to *sample multiple paths* simultaneously. Intuitively, SGD is a stochastic process with each path representing a sample of the possible outcomes. By sampling many paths we dramatically reduce the variance of the estimate.

This paper shows (in Section 2) that the following combiner achieves the two properties above:

$$\text{Adasum}(g_1, g_2) = \left(1 - \frac{g_1^T \cdot g_2}{2 \cdot \|g_1\|^2}\right)g_1 + \left(1 - \frac{g_1^T \cdot g_2}{2 \cdot \|g_2\|^2}\right)g_2$$

Here g_1 and g_2 are gradients from individual minibatches, $g_1^T \cdot g_2$ is their dot product, and $\|g\|^2$ represents the norm of the vector g . This combiner when recursively applied on gradients from all nodes generates a final gradient which can be used to update the starting model with an appropriate learning rate.

We call this approach Adasum as the combiner represents an adaptive sum of the two gradients with the gradients scaled by an appropriate constant.

Adasum achieves significant algorithmic efficiency with large batch sizes when compared to synchronous SGD by requiring far less number of epochs to converge to the same loss or model performance. This remains true even when using various learning-rate *optimizers*, such as Momentum-SGD [31], Adam [23], and LAMB [38]. Alternately, one can use the improved algorithmic efficiency to scale to a much larger effective batch size. For example, for Resnet50 Adasum enables Momentum SGD optimizer to converge with an effective batch size of 64K, which is four times larger than the largest batch size we have seen reported for Resnet50 as per MLPerf v0.5 submissions. Similarly, for BERT-Large, Adasum enables the Adam optimizer to scale to an effective batch size of 128K. Lack of convergence of Adam beyond 16K was the motivation for more sophisticated optimizers such as LARS and LAMB. When combined with LAMB, which is the state of the art optimizer for BERT-Large, Adasum converges in 20% fewer epochs than with LAMB alone when using an effective batch size of 64K. In addition, we demonstrate that LAMB with Adasum can also scale to 128K effective batch size. These results indicate that Adasum emulates the behavior of much smaller batch size even when running with large batch sizes.

A desirable property of the Adasum operation, as evident from the equation above, is that it has no hyperparameters. In all our experiments, we simply reused the recommended hyper-parameters for the baseline synchronous SGD. The only additional tuning Adasum entails is a search for suitable base learning rate.

In summary, the contributions of this paper are:

- Adasum, a new way to combine gradients that scales synchronous SGD to unprecedented batch sizes, and a proof of its convergence.
- A detailed discussion of how Adasum is implemented in Horovod, a popular distributed training framework for PyTorch and TensorFlow.
- An evaluation that demonstrates Adasum scales existing optimizers well beyond what was possible in prior work. For example, we demonstrate Adam can scale to 64K examples per allreduce on BERT (16K before), LAMB to 128K examples per allreduce on BERT (64K before), and Momentum-SGD to 64K examples per allreduce on ResNet-50 (16K before). All while maintaining downstream accuracy and with little hyper-parameter tuning.
- An evaluation that demonstrates for similar effective batch sizes as in prior work, Adasum converges faster than that prior work. For example, LAMB with Adasum on 64K examples per allreduce on BERT converges

in 30% fewer steps than LAMB when just averaging gradients.

2 Background

This section provides the background for the the paper, introducing notation and concept used throughout.

2.1 Stochastic Gradient Descent

Machine learning involves learning a model parameterized by a set of weights w based on some training data. Given a set of training examples $\{(x_1, y_1), \dots, (x_k, y_k)\}$ where each x_i is a vector representing the input instance i and y_i is its label, training involves finding a w that minimizes some loss function $L = \sum L_i(w, x_i, y_i)$, the sum of individual loss function L_i of the model w on input (x_i, y_i) .

Most training uses stochastic gradient descent (SGD). SGD starts from an appropriately initialized model w_0 and progressively updates the model at step i as $w_{i+1} = w_i - \alpha_i g_i$. Here α_i is the learning rate at this step as determined by a learning rate schedule, and $g_i = \frac{1}{b} \sum_{j=1}^b \nabla L_j(w_i)$ is the sum of gradients of individual loss functions for a randomly chosen *minibatch* of data of size b . The stochasticity of SGD arises because g_i is only an estimate of the true gradient of the loss function at w_i . For deep neural networks, the gradients can be computed by the backpropagation algorithm [16] that requires a forward and a backward evaluation of the model.

2.2 Synchronous SGD

As models get larger, training requires parallelizing them on distributed hardware. While there are other important sources of parallelism such as model parallelism and pipeline parallelism, these techniques are orthogonal to the data parallelism studied in this paper.

A common approach to data parallelism is *synchronous SGD*, where one computes the gradients for each dataset in a minibatch in parallel. This process works as follows. Each node processes a *microbatch* of data and computes its local gradient. The microbatch size is usually determined by the amount of memory available in the local node. Then a communication step sums up the local gradients from all nodes to compute the minibatch gradient. This process is called *allreduce*, after the MPI primitive that computes the sum of vectors from each node and stores the result in all the nodes. Optionally, each node can perform *gradient accumulation* to sum up multiple microbatches before communicating with other nodes. Adasum, the technique proposed in this paper, replaces allreduce for improved parallelism.

2.3 Algorithmic Efficiency vs System Efficiency

One way to increase data parallelism is to increase the minibatch size. However, this has the effect of reducing stochasticity of SGD resulting in reduced convergence. Thus, there is a delicate balance between parallelism and model performance in distributed ML training. To capture this tradeoff, we define two notions. *System Efficiency* represents the raw throughput of the system in the amount of training data processes per unit of time. Obviously, naively increasing the minibatch size will increase the system efficiency of synchronous SGD. *Algorithmic Efficiency* is the inverse of the amount of training data that needs to be processed in order to achieve some desired model accuracy. Increasing the minibatch size decreases the algorithmic efficiency requiring more data or equivalently more iterations/epochs on a given training dataset to achieve the same level of accuracy. In the worst case, training might not converge when minibatch size is increased beyond a certain threshold.

As one essentially cares about the training time to desired accuracy, the net accuracy of distributed training is a combination of system efficiency and algorithmic efficiency.

2.4 Learning Rate Optimizers

While one can naively use the resulting gradient to update the model, researchers have proposed various learning-rate *optimizers* that adaptively use different learning rates for different parts of the model. For instance, Adam [23] computes individual adaptive learning rates for different parameters based on the estimates of first and second moments of gradients. LARS [37] uses layer-wise adaptive learning rates for greater training stability. The recent LAMB optimizer [38] extends LARS to effectively train models like BERT with large minibatch sizes. The benefits of Adasum are orthogonal to and can be used in concert with these optimizers.

3 Adasum Algorithm

We present the intuitions behind the Adasum algorithm, while a mathematical treatment with convergence proof is in the Appendix.

Consider two nodes that respectively compute gradients g_1 and g_2 respectively on minibatches b_1 and b_2 . When using synchronous SGD, the effective gradient is the average $(g_1 + g_2)/2$. But as it is common to increase the learning rate proportional to the increased effective batch size, the combination amounts to a sum in practice. The main proposal behind this paper is to use an *adaptive sum* of the two gradients called the Adasum.

$$\text{Adasum}(g_1, g_2) = \left(1 - \frac{g_1^T \cdot g_2}{2 \cdot \|g_1\|^2}\right)g_1 + \left(1 - \frac{g_1^T \cdot g_2}{2 \cdot \|g_2\|^2}\right)g_2$$

Despite its apparent complexity, Adasum simply adds the two gradients after scaling with appropriate scalars. Using this operation instead of sum or average has the following two properties. First, the Adasum operation approximates the sequential execution of the two nodes running one after the other, thereby achieving convergence properties of smaller minibatch sizes. Additionally, it samples *both* possible orders of visiting minibatches — b_1, b_2 and b_2, b_1 . We then show how to extend the Adasum operation to more than two minibatches.

3.1 Emulating Sequential SGD

Consider two steps of SGD starting from model w_0 . Say, the first step computes a gradient $g_1(w_0)$ of the loss function at w_0 for b_1 . SGD updates the model to

$$w_1 = w_0 - \alpha \cdot g_1(w_0)$$

The second step computes its gradient $g_2(w_1)$ at w_1 for b_2 . Assuming we are using the same learning rate for both steps, the final model after the second step is

$$\begin{aligned} w_{1,2} &= w_1 - \alpha \cdot g_2(w_0) \\ &= w_0 - \alpha \cdot (g_1(w_0) + g_2(w_1)) \end{aligned} \tag{1}$$

Here the subscript for w indicates that SGD processed b_1 before b_2 . Comparing this what a synchronous SGD algorithm would have computed (with a corresponding doubling of the learning rate)

$$w_0 - \alpha \cdot (g_1(w_0) + g_2(w_0))$$

we see a difference because gradient g_2 is computed at w_0 instead of w_1 . As previously observed [24, 39], one can use second order reasoning to remove this staleness. Neglecting higher order terms in the Taylor expansion of $g_2(w_1)$, we have

$$g_2(w_1) = g_2 - \alpha \cdot H_2 \cdot g_1 \tag{2}$$

where H_2 is the Hessian matrix of the loss function at w_0 .

3.2 Eliminating Hyperparameters

One nice property of the standard synchronous SGD is that it adds no hyperparameters during gradient combination - we simply sum or average the two gradients. It is desirable to have the same property for Adasum. First, using a standard theorem [2, 18] for estimating the Hessian matrix for negative log likelihood loss functions (details in Appendix A.1), we can estimate

$$g_2(w_1) = g_2 - \alpha \cdot g_2 \cdot g_2^T \cdot g_1 \tag{3}$$

where for simplicity we have dropped the model term from g_1 and g_2 when computed at w_0 for terseness. This along with

the assumption that α is chosen optimally (Appendix A.2), we have

$$g_2(w_1) = g_2 - \frac{g_2^T \cdot g_1}{\|g_2\|^2} g_2 \quad (4)$$

Essentially, by scaling g_2 with an appropriate scalar, we can emulate the sequential execution of two SGD steps in Equation 1 as

$$w_{1,2} = w_0 - \alpha \cdot [g_1 + (1 - \frac{g_2^T \cdot g_1}{\|g_2\|^2}) \cdot g_2] \quad (5)$$

3.3 Sampling Multiple Paths

The ability to emulate a sequential execution shown above provides an intriguing possibility. SGD is a stochastic process that samples a *path* defined by the order of the training data it processes. Now, the emulation above provides us a way to sample multiple paths for the cost of one! For instance, if SGD had processed minibatch b_2 before b_1 , the final model would be

$$w_{2,1} = w_0 - \alpha \cdot [g_2 + (1 - \frac{g_2^T \cdot g_1}{\|g_1\|^2}) \cdot g_1]$$

Averaging the two samples, the final model would be

$$\begin{aligned} w_{1,2+2,1} &= w_0 - \alpha \cdot [(1 - \frac{g_2^T \cdot g_1}{2 \cdot \|g_1\|^2}) \cdot g_1 + (1 - \frac{g_2^T \cdot g_1}{2 \cdot \|g_2\|^2}) \cdot g_2] \\ &= w_0 - \alpha \cdot \text{Adasum}(g_1, g_2) \end{aligned}$$

This equation motivates our design of the Adasum operator.

3.4 Combining More Than Two Gradients

We can extend Adasum to more than two gradients by recursively applying the operator as follows. Let $g_{[0,n]}$ be the result of applying Adasum to minibatches $b_0 \dots b_n$. We can consider this as the *effective* gradient of these minibatches when emulating the behavior of SGD on b_{n+1} . Using the same arguments as above, we have

$$\text{Adasum}(g_{[0,n+1]}) = \text{Adasum}(\text{Adasum}(g_{[0,n]}), g_{n+1})$$

Since we double the number of paths of SGD emulated at each step, we achieve the effect of emulating *exponentially* many SGD paths.

As discussed in Section 4, one can reuse the standard ring algorithm used to sum all the gradients in synchronous SGD to implement the Adasum operation. One complexity is that the operation cannot be performed in a streaming manner as we need to compute the dot product and norm of the two gradients. For a more bandwidth optimal implementation, we use the following recursive application in practice.

$$\text{Adasum}(g_{[0,n]}) = \text{Adasum}(\text{Adasum}(g_{[0,n/2]}), \text{Adasum}(g_{[n/2,n]}))$$

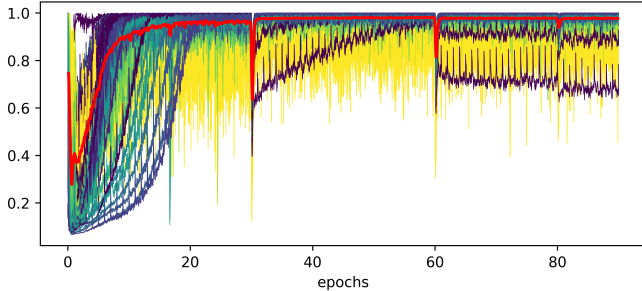
3.5 Adasum Properties

Consider $\text{Adasum}(g_1, g_2)$ when g_1 and g_2 are orthogonal. Their dot product $g_2^T \cdot g_1$ is zero. Therefore, Adasum simply adds the two gradients. Now consider the case when they are parallel. Their dot product is simply the product of their norms. So, Adasum becomes the average of the two gradients. Intuitively, when the two gradients are pointing in orthogonal directions, Adasum behaves as if their loss functions are locally independent and aggressively sums the two gradients. Doing so when the two gradients are parallel has the danger of "overshooting" the minimum, particularly when the learning rate is also aggressive and therefore, Adasum safely averages the gradients. This adaptiveness becomes important as we later show that gradients from different batches tend to point in the same direction during the initial parts of the training. This is because the initial model is completely random and all gradients agree on the general direction model should progress. However, the gradients become progressively orthogonal in later parts of the training. Adasum automatically and adaptively interpolates between an aggressive sum and a safe average as training proceeds.

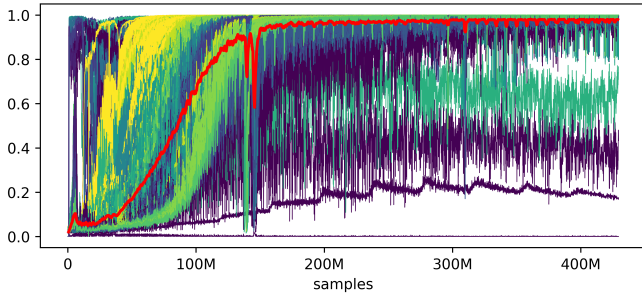
3.6 Per-Layer Orthogonality

For further insights, Figure 1 shows the per-layer orthogonality of gradients during training. At different points during the training of ResNet-50 and BERT-Large with 64 GPUs, we compared the norm of the result of Adasum on the gradients from individual layers across all 64 nodes with the individual norm of the gradients. Orthogonality of a set of gradients $g_1 \dots g_n$ for a given layer is defined as $\frac{\|\text{Adasum}(g_{[1,n]})\|^2}{\sum_i \|g_i\|^2}$. This compares the norm of the result of Adasum on a set of gradients with the sum of their individual norms. Because of the properties of Adasum described above, orthogonality is 1 when the gradients are orthogonal to each other and reaches the minimum value of 1/64 when the gradients are parallel to each other and are of the same norm. Of other ways of measuring orthogonality, this was the easiest for us to collect experimentally.

The figures 1a and 1b show the orthogonality of different layers and their average, shown by the bold red lines, for both ResNet-50 and BERT-Large. We can clearly see from the average of the orthogonality (red lines) that the gradients start out pointing in the same direction but very soon become orthogonal as the training proceeds. Each layer also demonstrate a similar pattern with a different color shown in Figure 1. Of course, there are too many layers to distinguish each color individually. However, general trends are still visible. While most layers tend to become orthogonal as training proceeds, they do not do so at the same rate. This discrepancy is more visible for BERT-Large, where some layers have low orthogonality throughout the training process. Note that, there are clear drops in the orthogonality during the training for both



(a) ResNet-50



(b) BERT-Large

Figure 1: Orthogonality of gradients during ResNet-50 (a) and BERT-Large (b). x-axis represents number of samples or epochs processed during training. A value of 1 in the y-axis means that the gradients are orthogonal with lower values meaning less orthogonality. The bold red lines show orthogonality averaged across all layers, while the others show the orthogonality of individual layers with different colors.

benchmarks. These drops happens exactly at boundaries of learning rate schedule change.

To exploit this observation, we perform the Adasum operation *per layer* as opposed to applying to the whole gradient. This allows us to adaptively adjust the combination based on per-layer orthogonality.

3.7 Evaluating Sequential Emulation

To validate our intuitions behind Adasum, we empirically evaluate how closely Adasum emulates a sequential emulation. As shown earlier in Equation 2, we can reduce the staleness of gradients using the Hessian of the loss function. Luckily, for small models such as LeNet-5, we can compute the Hessian matrix exactly. Specifically, we downloaded the PyTorch MNIST tutorial example, modified the code to ensure deterministic runs, and used PyTorch’s autograd facilities to compute the exact Hessian at each step during a parallel run with 64 nodes (that reached the target accuracy of 99.3%). After every communication step, we computed the model with sequential emulation using the exact Hessian, using the Adasum operator, and using the baseline synchronous SGD. Figure 2 shows the relative error of Adasum and synchronous SGD with respect to the sequential emulation using the Hes-

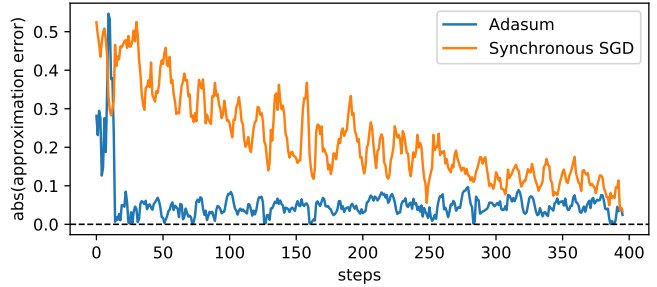


Figure 2: Relative error of Adasum and synchronous SGD when compared to a sequential emulation that uses the exact Hessian matrix.

sian. As we can see, Adasum has a lower approximation error reaching close to zero at some steps. Note synchronous SGD error goes down with number of steps—the reason is because the norm of gradients $\|g\|$ decays as the model approach the optimal answer and $H \approx g \cdot g^T$ decays quadratically. In a real run, the error shown here is accumulated during the training process. This further validates our intuition that Adasum should achieve faster convergence than synchronous SGD, which we demonstrate empirically in Section 5.

4 Implementation

Adasum is implemented in Horovod [3] and is publicly available in the main branch of its open-source repository. Horovod integrates with multiple machine learning frameworks, such as TensorFlow and PyTorch. Horovod has a C++ backend targeting multiple backend transports like Ethernet/IB or NVLINK. Adasum works with CUDA aware MPI (when available) and we implemented Adasum for all of these backends.

4.1 Using Adasum in Horovod

Adasum is easy to use by specifying an option to the DistributedOptimizer API of Horovod as follows.

```
opt = hvd.DistributedOptimizer(opt, op=hvd.Adasum)
```

When enabled, the distributed optimizer calls the necessary Adasum allreduce operations to synchronize global model updates. As with Horovod, the user is responsible for partitioning data across nodes and initializing the model correctly in all nodes.

Providing the option is the only change required for users wanting to use an existing DistributedOptimizer such as Adam or LAMB. For more fine grained control, we also expose the Adasum operator through Horovod’s allreduce using the same option.

```
hvd.allreduce(opt, op=hvd.Adasum)
```

```

params = list(model.parameters())

# save a copy of the model parameters
starts = [p.clone().detach() for p in params]

# do forward / backward
...

# optimizer step
optimizer.step() # modifies params

# apply adasum after optimizer
for start, current in zip(starts, params):
    effective_gradient = current - start
    hvd.allreduce(effective_gradient, op=hvd.Adasum)
    current.data.add_(effective_gradient)

```

Figure 3: Implementation of Adasum with optimizers such as Adam or LAMB.

This is useful when users want to perform additional operations such as gradient clipping beyond those implemented in a DistributedOptimizer.

One subtlety in the implementation is that the Adasum operation should be performed *after* the optimizer update, as shown in Figure 3. In contrast, synchronous SGD performs allreduce before the optimizer update. Intuitively, this is because Adasum does not increase the minibatch size like synchronous SGD when distributing across multiple nodes. As such, the logic of optimizers should only apply to the smaller minibatches per node. This is similar to BMUF [11]. Users have to replicate this logic explicitly when not using an existing DistributedOptimizer directly.

4.2 Adasum Allreduce Implementation

This section describes the implementation of the Adasum operator in Horovod’s allreduce. Message Passing Interface (MPI) provides capabilities to perform user-defined reduction operations for allreduce. However, since these custom reductions can only be elementwise, Adasum cannot be implemented as a user-defined reduction.

4.2.1 Recursive Vector-Halving

Our implementation of Adasum uses a modified recursive vector-halving (RVH) algorithm for allreduce [10, 35], which is both latency and bandwidth optimal in a hypercube and fully connected networks. On each step of the reduce-scatter phase of the algorithm each node exchanges half of its data with its neighbor and applies the reduction on its own half. In the baseline algorithm, since each application of the reduction operation is only given a part of the data, the operation must be elementwise to ensure the correct result.

Algorithm 1 Recursive vector-halving with Adasum

Require: $size > 2$ is a power-of-two.

```

1: procedure ADASUMRVH( $x, d$ )
2:    $mid = \lfloor |x|/2 \rfloor$ 
3:   if  $\lfloor rank/d \rfloor$  is even then ▷ Left neighbor
4:      $nghr = rank + d$ 
5:      $SEND(x_{mid:|x|}, nghr)$  ▷ Send right half
6:      $a = x_{0:mid}$ 
7:      $b = RECV(nghr)$  ▷ Receive left half
8:   else ▷ Right neighbor
9:      $nghr = rank - d$ 
10:     $SEND(x_{0:mid}, nghr)$  ▷ Send left half
11:     $a = RECV(nghr)$  ▷ Receive right half
12:     $b = x_{mid:|x|}$ 
13:  end if
14:   $d' = 2 \cdot d$ 
15:   $v = [a \cdot b, a \cdot a, b \cdot b]$  ▷ Partial dot products
16:   $group = [\lfloor \frac{rank}{d'} \rfloor \cdot d' + i \text{ for } i = 0 \dots d' - 1]$ 
17:   $v = ALLREDUCE(v, +, group)$  ▷ Finish dot products
18:   $x' = a \cdot (1 - \frac{v_1}{2v_2}) + b \cdot (1 - \frac{v_1}{2v_3})$  ▷ Apply Adasum
19:  if  $d' < size$  then
20:     $x' = ADASUMRVH(x', d')$ 
21:  end if
22:   $SEND(x', nghr)$  ▷ Send my half
23:   $y = RECV(nghr)$  ▷ Receive neighbor’s half
24:   $x = x' ++ y$  if  $\lfloor rank/d \rfloor$  is even else  $y ++ x'$ 
25: end procedure

```

To work around this problem we modify the RVH algorithm to perform each Adasum operation in two phases, with an additional step of communication in between. Algorithm 1 describes these modifications. Each process is identified by a zero-based index called rank. A process can send a vector v to another rank r with $SEND(v, r)$ and receive one with $v = RECV(r)$. The algorithm also uses another allreduce as a primitive to sum partial dot products and squared norms across subgroups of ranks: $ALLREDUCE(v^i, op, group)$ returns a pointwise reduction of vectors v_i from all ranks $i \in group$, where $group$ is a list of the ranks participating in the reduction

Each level of recursion in Algorithm 1 starts with ranks exchanging half of their vector x with a neighbor at distance d (lines 2-13). Here the two halves a and b are assigned such the left neighbor’s half is in a and the right neighbor’s half is in b .

Lines 15-18 of Algorithm 1 represent the main modification to baseline RVH algorithm. First, on line 15, each rank calculates a dot product and squared norms for a and b , which are slices of a larger logical vector shared across exactly the ranks in $group$ (line 16). Line 17 then sums the products among the ranks in $group$ to produce the complete results in v . The reduction is finally applied locally using the values in

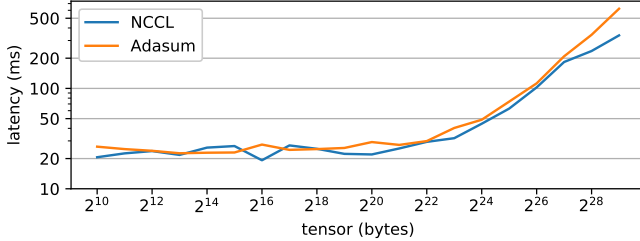


Figure 4: Latency of ADASUMRVH vs. NCCL for various message sizes.

v (line 18).

The algorithm continues as normal, using recursion on line 20 until all ranks share slices of the same reduced vector, followed by an all-gather phase on lines 22-24.

4.2.2 Integration into Horovod

Horovod uses ADASUMRVH to reduce tensors whenever `hvd.allreduce` or `hvd.DistributedOptimizer` is used with `op=hvd.Adasum`. Additionally, if the `HOROVOD_HIERARCHICAL_ALLREDUCE` environment variable is set Horovod performs a *hierarchical* allreduce using the NVIDIA Collective Communications Library (NCCL). This variant starts and ends with a NCCL reduce-scatter and allgather, respectively, for communication among the GPUs inside a node, with cross-node reduction handled by ADASUMRVH. This is useful with some hardware configurations on which NCCL offers higher throughput than CUDA-aware MPI.

4.2.3 ADASUMRVH Performance

Now we evaluate the latency of ADASUMRVH on 16 Azure nodes with 4 V100s per node (PCIe interconnect) and a single 100 Gb/s Infiniband connection between them. As a baseline, we compare to NCCL's sum operation. A point on Figure 4 (x,y) shows the latency for an allreduce operation (y) in seconds as a function of the number of bytes reduced (x). For each point on the x axis, we allocate 64 tensors on each GPU's memory so their sum is the the number of bytes. The figure demonstrates that despite the additional logic required to perform an adaptive summation, the performance of *RVHAdasum* is roughly equal to the highly optimized NCCL library simply doing a summation. Note that these results use vectorization as well as tensor fusion with a threshold of 2MB as discussed in Section 4.4.2 and 4.4.3.

As section 3.4 described, there are two ways of applying the pairwise Adasum operation on a set of gradients. ADASUMRVH performs the "tree" reduction. An alternate way is to apply the Adasum operator linearly. We additionally implemented this approach and optimized it using techniques similar to the ring allreduce algorithm commonly used for

synchronous SGD. We found that this "ring" implementation provided less throughput than the baseline NCCL allreduce and ADASUMRVH on the architectures we evaluated. Nevertheless, we believe the ring allreduce version of Adasum could be competitive for other architectures.

4.3 Parallelizing Adasum Computation

For large models such as BERT-Large, memory available in a GPU only fits a small microbatch size. In such cases, to increase the effective microbatch size, we use the GPUs available in a single node to accumulate local gradients and use the Adasum operation across nodes. In these scenarios, we parallelize the Adasum computation across all these local GPUs.

Our approach is inspired by the optimizer-state partitioning algorithm pioneered by Marian [4], a deep learning toolkit optimized for NLP workloads. Optimizers like Adam or LAMB maintain additional state per gradient element to estimate moving mean and/or variance. The optimizer parameters are identical for all GPUs and thus it is not necessary to replicate them. Marian partitions this state and parallelizes the updates to the state. Note that this memory optimization is not related to model parallelism as model parameters are still replicated on all GPUs.

We use the same insight to parallelize the Adasum computation. Looking at Figure 3, we partition the optimizer state as in Marian. In addition, we also partition the `effective_gradient` across the local GPUs. A key difference between the Marian approach is that rather than distributing this state uniformly, we partition to ensure that state corresponding to one neural network layer falls in the same partition. This greatly simplifies our implementation as we do not have to modify the code of the underlying optimizer.

After the optimizer update, which is done in parallel (as in Marian), the `effective_gradient` in Figure 3 is already partitioned across local GPUs. Now, each GPU does an Adasum allreduce only on the layers in its partition by communicating with the corresponding GPU that share partitions in other nodes. Finally, the GPU broadcasts its partition of `effective_gradient` locally to all other GPUs in the same node to update the model parameters. To optimize the cost of this local broadcast, we overlap this communication with the Adasum operation of the next layer.

| | Without | With |
|------------------------|---------|-------|
| Throughput (samples/s) | 154.7 | 168.5 |
| Model update (s) | 1.82 | 0.97 |
| Microbatch | 22 | 36 |

Table 1: Performance improvement with and without Adasum parallelization.

The table above shows the performance improvement of

this optimization for a PyTorch implementation of BERT-Large on a Azure VM with 4 V100s (16 GB RAM) connected by PCIe for 128 max sequence length. Since this optimization reduces the memory usage, we can increase the microbatch size by 60% as shown in the last column. To measure the impact of this larger microbatch, we evaluate 256 microbatches before an adasum operation. The first column in Table 1 provides the throughput per GPU. In other words, the 60% larger microbatch yields nearly a 10% improvement in per GPU throughput. To measure the impact of parallelizing the Adasum operation, we evaluate a microbatch size of 1 per model update. The third column in Table 1 shows that this time drops nearly $1.87\times$.

4.4 Implementation Details

This section describes implementation details that are crucial for improving system and algorithmic efficiency of Adasum.

4.4.1 Low Precision Support

Recent trends in ML training have shown the promise of using low-precision formats such as fp16 for compute and communication efficiency. Our implementation of Adasum integrates with the low-precision support in Horovod to obtain these benefits automatically.

We discuss two important subtleties in our implementation of low-precision support. First, Adasum requires computing the dot product and norms of the combined gradients. The accumulation of the values for these two operations happens in a double even if the gradients are in lower precision. This does not incur any measurable overhead for both CPU and GPU implementations. On the other hand, the improved floating point stability is crucial for the improved convergence of Adasum.

When using lower-precision, it is common to use *dynamic scaling* [25]. The basic idea is to maintain a *scale* for all tensors to ensure that the values are always in the dynamic range of the low-precision format. During the training, these scales have to be periodically adjusted when the values exceed the range (resulting in nans). We perform dynamic scaling for tensors we introduce, such as the `effective_gradient` in Figure 3.

4.4.2 CPU and GPU Vectorization

Adasum runs on both CPU and GPU hardware in fp16, fp32, and fp64. For CPU hardware, we manually vectorize loop bodies that perform both dot products and summations. When Horovod is compiled with CUDA aware MPI, we implement these same loops as GPU kernel calls that operate directly on GPU memory and thus save on the transfer from GPU to CPU. This is particularly important on hardware that supports GPUDirect RDMA as GPU memory need not be copied to the CPU for the Adasum operator.

4.4.3 Tensor Fusion

If at the time of allreducing a tensor, tensors from other layers are also ready and available on all hosts, Horovod fuses these tensors into a single one, performs an allreduce on the fused tensor, and then copies from the fused tensor back to the individual tensors. This optimization significantly reduces latency for small tensors as the overhead of potentially many individual allreduce calls are amortized into a single one. To enable this optimization with Adasum, we do additional bookkeeping to keep track of tensor boundaries in the fused tensor as Adasum requires these boundaries to compute dot products per layer. Because all hosts 1) fuse the same set of tensors and 2) have the same layer sizes, this bookkeeping is stored locally and does not increase communication overheads. Note that Horovod uses an extra buffer for copying the tensors from different layers into a consecutive array so that underlying libraries such as MPI or NCCL can be called once. Adasum uses the same buffer for this optimization. The size of this buffer is controlled by `HOROVOD_FUSION_THRESHOLD`. A default value between 2MB-64MB usually works well.

5 Results

To show that Adasum works across a variety of real-world training scenarios, we evaluate its performance through a sequence of case studies. Throughout the experiments, we use our implementation of Adasum in Horovod described in Section 4 on models implemented in both PyTorch and TensorFlow.

We first study the algorithmic and system efficiency of Adasum for ResNet-50 and BERT-Large. Then, we use LeNET5, which is small enough to do extensive hyperparameter tuning, to show that Adasum enables robust scaling without the need for additional hyperparameter tuning. Finally, we finish with a short summary of our experience with production models.

5.1 ResNet-50 on Fast Interconnects

This section evaluates Adasum on PyTorch’s ResNet-50 using the Momentum-SGD optimizer on hardware with a fast interconnect.

5.1.1 Platform and Methods

ResNet-50 [19] on Imagenet [32] is a popular model for studying performance of training algorithms and implementations. We used PyTorch’s ResNet-50 model modified to run with Horovod and compared the performance of Adasum with Horovod’s default *Sum* operator as the baseline for synchronous SGD. We ran experiments on Azure’s Standard_NC24rs_v3 virtual machines, each of which has 4 NVIDIA Tesla V100 GPUs connected with PCIe, dual-socket

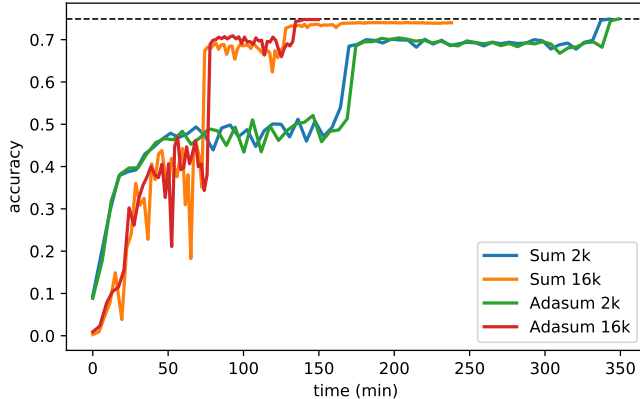


Figure 5: Time-to-accuracy chart for ResNet-50 with 64 GPUs on 16 Standard_NC24rs_v3 VMs.

Intel Xeon E5-2690 v4 CPUs, 448 GiB of memory, and connected via Infiniband. Hierarchical allreduce, as described in Section 4.2.2 was faster for both the baseline and Adasum runs so we used it here.

We train on 64 V100s with 2K and 16K examples per allreduce and use the default hyper-parameters that ship with the benchmark for its momentum based SGD optimizer.

5.1.2 Algorithmic Efficiency

The number of epochs required for each configuration to reach the target accuracy are as follows:

| Sum 2k | Sum 16k | Adasum 2k | Adasum 16k |
|--------|---------|-----------|------------|
| 62 | - | 62 | 69 |

Because sum with 16k batch size *never* reaches 74.9% validation accuracy (we let it run for 120 epochs), its algorithmic efficiency is zero. Adasum on the other hand sees only a 11% decline in its algorithmic efficiency as we increased the batch size. This is more than made up for in increased system efficiency.

5.1.3 System Efficiency

The times per epoch for each configuration are as follows:

| Sum 2k | Sum 16k | Adasum 2k | Adasum 16k |
|----------|----------|-----------|------------|
| 5.61 min | 2.12 min | 5.72 min | 2.23 min |

Adasum closely matches the system efficiency of Horovod’s sum implementation at both 2k and 16k batch size. Increasing the batch size from 2k to 16k results in a 61% and 62% improvement for Adasum and sum, respectively.

The total efficiency can be seen in Figure 5, which shows the time (x -axis) to accuracy (y -axis) for each configuration. Sum 16k plateaus below the target accuracy. Adasum 16k, on the other hand, gets to a top-1 accuracy of 74.9%, being 2.3X faster in time to accuracy than Adasum 2k, *while using the same number of GPUs*.

| | | |
|----------------------------------|--------|--------|
| Local steps before communicating | 16 | 1 |
| Effective batch size | 64K | 4K |
| Minutes per epoch | 1.98 | 2.58 |
| Epochs till convergence | 84 | 68 |
| Time to accuracy(min) | 166.32 | 175.44 |

Table 2: Algorithmic and System efficiency for TensorFlow ResNet-50 on TCP. Adasum enables faster time to accuracy by doing more compute per communication.

5.2 TensorFlow ResNet-50 on Slow TCP

Horovod and Adasum run on all types of hardware. Often, networks have TCP rather than IB and as such, communication limits scaling to multiple nodes. This section demonstrates Adasum enables a larger effective batch size, which reduces communication overhead, and yet still converges fast enough to reduce time to accuracy.

5.2.1 Platform and Methods

This section demonstrates how a TensorFlow implementation of ResNet-50 from MLPerf’s v0.5 reference implementation [5] is able to scale to 16 V100s (4 GPUs 32GB cards per node with a PCIe gen 3 interconnect) and TCP (40 GB/s) interconnects in between.

We downloaded the MLPerf v0.5 reference implementation and slightly modified it to use Horovod with Adasum. We did a small hyper-parameter search over the learning rate but did not change any other hyper-parameters. We found $4\times$ the default learning rate provided the fastest convergence. This benchmark uses the Momentum SGD optimizer from TensorFlow. MLPerf v0.5 converges when the test accuracy is greater than or equal to 74.9%.

Unlike simply adding the gradients together for gradient accumulation, the TensorFlow Adasum enabled distributed optimizer uses a local SGD step to update weights; when it is time for an allreduce, the gradient is estimated via a delta from the model’s state since the prior allreduce.

5.2.2 Algorithmic Efficiency

Table 2 shows the results of this experiment. Adasum for TensorFlow enables a form of gradient accumulation where the toolkit makes many local steps before communicating. The first row denotes how many local steps to make before initiating an allreduce with the Adasum operation. Note that when it takes 1 local step before communicating, there is no gradient accumulation. In contrast, 16 local steps before communicating means that the allreduce is called once every 16 local steps. With 16 GPUs and 256 examples per GPU, the convergence is fast in 68 epochs (fourth row in Table 2). That convergence slows to 84 epochs with an effective batch size of 64K. It is important to note that none of the submissions to

MLPerf v0.5 used more than a 16K effective batch size (we verified by looking at the result submissions). Thus Adasum is able to scale the TensorFlow momentum optimizer to 64K examples before communicating $4\times$ more than prior art.

5.2.3 System Efficiency

When communicating after every step, the system efficiency is low as communication dominates (third row in Table 2). In contrast, when we communicate every 16 local steps, the time for 1 epoch is much faster. Total running time is given by the last row: min per epoch * epochs till convergence and clearly communicating less frequently has a big impact in overall running time despite the slight increase in algorithmic efficiency. Thus, a developer can exploit fast distributed hardware even without a fast interconnect.

5.3 BERT-Large

This section shows Adasum scales both Adam [22] and LAMB [38] for the PyTorch NVIDIA implementation of BERT-Large [7].

5.3.1 Platform and Methods

Training BERT-Large [14] a natural language processing (NLP) model, takes place in two stages. First is an unsupervised *pre-training* on two large text corpuses, Wikipedia and BookCorpus. Then, the model is fine-tuned for a “downstream” NLP task such as SQuAD question-answering [28, 29]. A target F1 score of SQuAD 1.1 of 90.5 averaged over 5 tries with different seeds is generally accepted for BERT-Large pre-training [14, 38].

Pre-Training BERT-Large requires tokenizing input sentences into a max sequence length. A maximum sequence length of 512 is computationally expensive and thus Devlin *et al.* suggest [14] breaking pre-training into two phases: phase 1 with a maximum sequence length of 128 for 90% of the training iterations and phase 2 with a maximum sequence length of 512 for the remaining 10%.

NVIDIA’s repo contains scripts that 1) download and pre-process data, 2) phase 1 and 2 pre-training and, 3) SQuAD fine-tuning and evaluation. NVIDIA’s pre-training scripts use mixed precision training in addition to data parallelism with NCCL [6]. This codebase is our baseline and for the Adasum implementation, we replaced its use of `torch.distributed` with the Adasum operator in Horovod.

The system that we used for this case study is a cluster of DGX-2 nodes where each node has 16 V100 GPUs with 32GB of memory per GPU and NVSwitch intra connection. Each node has 8 NICs with Infiniband support capable of delivering a throughput of 800GB/s per node.

| Algorithm | Number of iterations | |
|--------------------|----------------------|---------|
| | Phase 1 | Phase 2 |
| Baseline-Adam | - | - |
| Baseline-LAMB [38] | 7039 | 1563 |
| Adasum-Adam | 7039 | 1563 |
| Adasum-LAMB - 20% | 5639 | 1250 |
| Adasum-LAMB - 30% | 5039 | 1563 |
| Adasum-LAMB - 128K | 4574 | 1563 |

Table 3: Algorithmic efficiency results on BERT-Large. Table shows the number of iterations required for Phase 1 and Phase 2 to achieve target SQuAD score of 90.5, when using the effective batch size of 64K for Phase 1 and 32K for Phase 2.

5.3.2 Algorithmic Efficiency

Table 3 describes the algorithmic efficiency of Adasum over the Adam and LAMB optimizer when using an effective batch size of 64K for Phase 1 and 32K for Phase 2. As reported in prior work, the Adam optimizer does not scale to batch sizes beyond 16K. This motivated the study of more sophisticated optimizers such as LARS and LAMB. For instance, our runs of the LAMB optimizer achieve the target SQuAD score with 7039 iterations of phase 1 and 1563 iterations of phase 2, as shown in second row of Table 3.

The next two rows of Table 3 show the performance of Adasum. In contrast to Adam baseline, the Adasum-Adam optimizer converges with 64K when run with the same number iterations for Phase 1 and Phase 2 as the LAMB baseline. This is an interesting result as despite the advances of optimizers such as LAMB, Adam optimizer continues to be popular for some models. When compared to prior work [38], it is important to note that Adasum adds no additional hyperparameters simply reusing the baseline parameters of the Adam optimizer. On the other hand, improvements provided by Adasum are orthogonal to improvements in optimizers. As shown in Table 3, Adasum-LAMB provides close to 20% faster convergence compared to LAMB baseline requiring 5639 iterations for phase 1 and 1250 iterations phase 2.

We also performed two variations of our Adasum-LAMB results. First, we aggressively reduce the number of Phase 1 iterations by 30%. With an equivalent aggressive reduction on Phase 2, we slightly missed the target SQuAD score by 0.5. However, we did achieve the target accuracy with the full 1563 iterations in Phase 2, which is what we report in the table. With a more fine grained search for Phase 2 iterations, we believe we can achieve the target SQuAD score with fewer Phase 2 iterations. These results are still interesting as Phase 1 takes a larger percentage of training time than Phase 2.

For the second variation, we increased the effective batch size of Phase 1 to 128K. We were able to achieve the target SQuAD score with 4574 Phase 1 iterations, while using the standard 1563 iterations of Phase 2 with 32K batch size. To the best of our knowledge, this is the largest report effective

| GPUs | PH1 speedup | | PH2 speedup | | Time (minutes) | |
|------|-------------|--------|-------------|--------|----------------|--------|
| | Sum | Adasum | Sum | Adasum | Sum | Adasum |
| 64 | 1 | 0.98 | 1 | 0.99 | 997 | 809 |
| 256 | 3.79 | 3.61 | 3.89 | 3.92 | 260 | 214 |
| 512 | 7.47 | 6.48 | 7.24 | 7.28 | 135 | 118 |

Table 4: System efficiency on BERT-Large for an effective batch size of 64K and 32K for phase 1 and phase 2, respectively. The speedup numbers are relative to the throughput of Baseline-LAMB with 64 GPUs, which is 12.2K examples per second for Phase 1 and 4.6K examples per second for Phase 2. The improved convergence time of Adasum is a result of the 20% improvement in algorithmic efficiency as shown in Table 3.

batch size for BERT-Large.

5.3.3 System Efficiency

The algorithmic efficiency of Adasum is only useful if the algorithm can be implemented without substantial degradation in system efficiency. Table 4 shows the speedup of Adasum-LAMB when compared to Baseline-LAMB for an effective batch size of 64K. On our GPU cluster, the Baseline-LAMB processes 12.2K examples per second during Phase 1 and 4.6K examples per second during Phase 2. This reduction in throughput arises because Phase 2 has more computation due to increases sequence length. The speedup numbers in the table are relative to this baseline. For instance, at 256 GPUs, the baseline scales to a speedup of 3.789 (a perfect scaling would be 4). Just as a comparison with published NVIDIA numbers [7], the baseline finishes BERT-Large in 260 minutes which is slower than 236 minutes reported by NVIDIA. This difference is due to the NVIDIA cluster having a slightly more performant DGX-2H configuration using a higher clock speed compared to our DGX-2 cluster.

Though Adasum performs more computation during allreduce, the reduction in throughput for 64 GPUs is less than 2% for Phase 1 and less than 1% for Phase 2. As we increase the number of GPUs, the additional computation results in lower scaling efficiency for Phase 1. For instance, Adasum incurs roughly a 5% reduction (13% reduction) in throughput when compared to the baseline for Phase 1 on 256 (512) GPUs. On the other hand, the throughput for Phase 2 with Adasum shows similar scalability as the baseline as we increase the number of GPUs, with Adasum being faster sometimes. This is due to the fact that Phase 2 does more computation.

The reduction in system efficiency is more than compensated by the 20% reduction in algorithmic efficiency. As such, Adasum achieves faster time to accuracy than the baseline. In particular, Adasum completes BERT-Large in 214 minutes, which is faster than NVIDIA reported numbers on 256 GPUs [7]. On 512 GPUs, Adasum reaches the desired accuracy in 118 minutes. We observed some of the overhead is

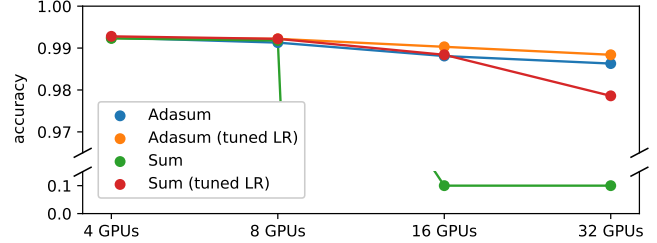


Figure 6: LeNet-5 accuracies under an aggressive sequential learning rate schedule for various distributed configurations.

due to CUDA aware MPI (openmpi + ucx) was not as fast as NCCL. We are in the process of porting Adasum’s allreduce to NCCL as a consequence.

5.4 Case Study: LeNet-5

LeNet-5 is a model for the MNIST dataset that is commonly used as a tutorial for neural networks. This pioneering image recognition model is very small by today’s standards. While speeding up training of LeNet-5 is not a priority, a benefit of evaluating Adasum on it is that *it is practical to do exhaustive hyperparameter search*. This allows us to thoroughly explore the convergence properties of Adasum using the following experimental setup. First, we will find a very aggressive learning rate schedule for sequential training that barely reaches a baseline accuracy. Now, keeping the number of epochs fixed, we can compare different distributed training configurations by how far off they are from the sequential accuracy.

We used the PyTorch version of LeNet-5 found in Horovod’s examples with a momentum based SGD optimizer with a batch size of 32. While the original example has a fixed learning rate schedule of 10 epochs, we were able to bring this down to 2 epochs using a linear warmup and decay from zero to zero.

The maximum accuracy of LeNet-5 on MNIST is in the 99.3%-99.4% range. Using 99.3% as our target accuracy, we used an Azure cluster of NC-series VMs with 333 NVIDIA K80 GPUs to optimize the hyperparameters of the training script. The following configuration reliably reaches the target accuracy in sequential training in 2 epochs (while no reliable configuration was found for 1.75 epochs):

| Epochs | Max LR | Warmup % |
|--------|--------|----------|
| 2 | 0.0328 | 17% |

We keep the number of epochs constant in the following experiments. Since MNIST has 60000 images, one GPU will take 1875 steps per epoch, while 32 GPUs would take only 58 steps per epoch.

We evaluated Adasum and Sum on 4, 8, 16 or 32 GPUs with both an unmodified learning rate as well as an optimized one, which we searched for separately for each combination of

method and number of GPUs. Figure 6 shows the accuracies reached by each configuration under the aggressive learning rate schedule for sequential training.

Without learning rate tuning Sum fails to converge at more than 8 GPUs, while Adasum still converges at 32 GPUs *without any hyperparameter search*. This highlights the easy scalability that Adasum enables. Furthermore, even with a tuned learning rate Sum is far below even untuned Adasum at 32 GPUs, and is still beat by Adasum with a tuned learning rate at 16 GPUs.

Consider the tuned learning rates for each configuration:

| Method | 4 GPUs | 8 GPUs | 16 GPUs | 32 GPUs |
|--------|--------|--------|---------|---------|
| Adasum | 0.0328 | 0.0147 | 0.012 | 0.0204 |
| Sum | 0.0275 | 0.017 | 0.0089 | 0.0043 |

For Sum going from 16 to 32 GPUs is coupled with a halving of the learning rate, which means that the per iteration step size stays the same even though twice as many GPUs are participating in each iteration. In contrast, Adasum can maintain much higher learning rates at 16 and 32 GPUs.

5.5 Case Study: Production Models

The prior case studies demonstrate the efficacy of Adasum on public models. Over the past three years, we have applied Adasum to a variety of production models from Company X¹ and observed similar improvement in convergence with little or no hyperparameter tuning. Due to space constraints, we only provide a summary of these results to show the broad applicability of Adasum. For instance, the team relying on an LSTM-based model for predicting the next command a user is likely to issue in an application was able to use Adasum to train on four times the amount of data to result in 6% improvement in downstream accuracy. Similarly, for a speech translation model with the Momentum optimizer, Adasum allowed the team to scale to 16 GPUs dramatically reducing the turn around time for their engineers. On a GPT-2 based model modified to work with code, Adasum provided 15% faster time to accuracy.

6 Related Work

Previous works for enabling large-batch training have focused on the problem of adapting the learning rate appropriately. This is helpful because while large batch sizes permit taking larger steps in many situations, the appropriate learning rate changes during training. Adam [23] adjust the step size based on the variance of gradients, taking smaller steps when variance is high. LARS [37] adapts learning rates per-layer using a *trust ratio* calculated as the ratio between the norm of the layer weights and the norm of gradients, the intuition being that divergence happens when steps are large in relation

¹Name removed for anonymity.

to the parameters being updated. LAMB [38] can be seen as LARS applied to Adam instead of vanilla SGD. These approaches that use statistical measures to adapt learning rate are qualitatively different from Adasum, which exploits a specific property (orthogonality) of gradients to take bigger steps when appropriate. Adasum and learning rate adaption methods are in many cases complementary, as we have shown in our experiments successfully combining Adasum with Adam and LAMB.

Asynchronous SGD [12, 13] approaches can address two issues in distributed synchronous SGD: synchronization overhead of faster nodes having to wait for stragglers to finish the iteration, and non-overlapping of compute and communication. However, stale gradients present another potential source of degraded convergence. Specifically, the DC-ASGD algorithm [39] addressed this staleness using an approximation of the Hessian as used in Adasum. They only use the diagonal elements of the $g \cdot g^T$ approximation of the Hessian and require an additional hyperparameter which requires a careful tuning over time. It was also only evaluated for SGD and Momentum-SGD. Our approach was motivated to be a drop-in replacement of the allreduce operation and thus we eliminate all hyperparameters in our combination and it is optimizer agnostic. Similarly, Maleki et al. [24] use the Hessian to reduce staleness and use a Johnson-Lindenstrauss projection to get a low rank approximation of a semantics-preserving model combiner. Their approach only works with exact Hessian computation and is unlikely to scale to DNNs.

While large-batch training methods decrease the amount of communication needed, *gradient compression* approaches reduce the cost of each communication round. In gradient quantization approaches gradients are cast to a lower bit-width datatype for communication, with bit-widths ranging all the way down to 1 bit [33]. Low-rank compression methods communicate the most important dimensions of gradients [36]. Any lossy gradient compression presents yet another potential source for loss of convergence.

7 Conclusion

Adasum unlocks an unprecedented level of scalability for data parallel distributed training of large models. Our case studies show that Adasum scales BERT-Large-LAMB to 128k batch size, BERT-Large-Adam to 64K batch size, and ResNet-50 Momentum to 64k batch size, while maintaining downstream accuracy. Adasum is publicly available through open-source Horovod package [3], can be simply enabled with an additional flag, and requires no additional hyper-parameters.

Finally, Adasum opens a new direction for future work on lightweight ways to exploit orthogonality in model updates. We expect Adasum’s empirical observations to drive future work in adaptive learning rate methods and further communication optimizations.

References

- [1] Cloud tpu. <https://cloud.google.com/tpu>. Accessed: 2020-05-22.
- [2] Fisher information and the hessian of log likelihood. <http://mark.reid.name/blog/fisher-information-and-log-likelihood.html>. Accessed: 2020-05-22.
- [3] Horovod: Overview. https://horovod.readthedocs.io/en/latest/summary_include.html. Accessed: 2020-05-22.
- [4] Marian: Fast neural machine translation in c++ <https://marian-nmt.github.io>. Accessed: 2020-05-22.
- [5] Mlperf: Fair and useful benchmarks for measuring training and inference performance of ml hardware, software, and services. <https://mlperf.org/>. Accessed: 2020-05-22.
- [6] Nccl: The nvidia collective communications library. <https://docs.nvidia.com/deeplearning/nccl/user-guide/docs/overview.html>. Accessed: 2020-05-22.
- [7] Nvidia deep learning examples for tensor cores. <https://github.com/NVIDIA/DeepLearningExamples>. Accessed: 2020-05-22.
- [8] Nvidia dgx-1. <https://www.nvidia.com/en-us/data-center/dgx-1/>. Accessed: 2020-05-22.
- [9] Nvidia dgx-2. <https://www.nvidia.com/en-us/data-center/dgx-2/>. Accessed: 2020-05-22.
- [10] Ernie Chan, Marcel Heimlich, Avi Purkayastha, and Robert van de Geijn. Collective communication: theory, practice, and experience. *Concurrency and Computation: Practice and Experience*, 19(13):1749–1783, 2007.
- [11] Kai Chen and Qiang Huo. Scalable training of deep learning machines by incremental block training with intra-block parallel optimization and blockwise model-update filtering. In *ICASSP-2016*, March 2016.
- [12] Trishul Chilimbi, Yutaka Suzue, Johnson Apacible, and Karthik Kalyanaraman. Project adam: Building an efficient and scalable deep learning training system. In *11th USENIX Symposium on Operating Systems Design and Implementation (OSDI 14)*, pages 571–582, Broomfield, CO, October 2014. USENIX Association.
- [13] Jeffrey Dean, Greg Corrado, Rajat Monga, Kai Chen, Matthieu Devin, Mark Mao, Marc'aurelio Ranzato, Andrew Senior, Paul Tucker, Ke Yang, Quoc V. Le, and Andrew Y. Ng. Large scale distributed deep networks. In F. Pereira, C. J. C. Burges, L. Bottou, and K. Q. Weinberger, editors, *Advances in Neural Information Processing Systems 25*, pages 1223–1231. Curran Associates, Inc., 2012.
- [14] Jacob Devlin, Ming-Wei Chang, Kenton Lee, and Kristina Toutanova. BERT: Pre-training of deep bidirectional transformers for language understanding. In *Proceedings of the 2019 Conference of the North American Chapter of the Association for Computational Linguistics: Human Language Technologies, Volume 1 (Long and Short Papers)*, pages 4171–4186, Minneapolis, Minnesota, June 2019. Association for Computational Linguistics.
- [15] Li Dong, Nan Yang, Wenhui Wang, Furu Wei, Xiaodong Liu, Yu Wang, Jianfeng Gao, Ming Zhou, and Hsiao-Wuen Hon. Unified language model pre-training for natural language understanding and generation. In *33rd Conference on Neural Information Processing Systems (NeurIPS 2019)*, December 2019.
- [16] Ian Goodfellow, Yoshua Bengio, and Aaron Courville. *Deep Learning*, chapter 6.5, page 200–220. MIT Press, 2016. <http://www.deeplearningbook.org>.
- [17] Priya Goyal, Piotr Dollár, Ross B. Girshick, Pieter Noordhuis, Lukasz Wesolowski, Aapo Kyrola, Andrew Tulloch, Yangqing Jia, and Kaiming He. Accurate, large minibatch SGD: training imagenet in 1 hour. *CoRR*, abs/1706.02677, 2017.
- [18] Trevor Hastie, Robert Tibshirani, and Jerome Friedman. *The Elements of Statistical Learning*. Springer Series in Statistics. Springer New York Inc., New York, NY, USA, 2001.
- [19] K. He, X. Zhang, S. Ren, and J. Sun. Deep residual learning for image recognition. In *2016 IEEE Conference on Computer Vision and Pattern Recognition (CVPR)*, pages 770–778, 2016.
- [20] Elad Hoffer, Itay Hubara, and Daniel Soudry. Train longer, generalize better: closing the generalization gap in large batch training of neural networks. In I. Guyon, U. V. Luxburg, S. Bengio, H. Wallach, R. Fergus, S. Vishwanathan, and R. Garnett, editors, *Advances in Neural Information Processing Systems 30*, pages 1731–1741. Curran Associates, Inc., 2017.
- [21] Nitish Shirish Keskar, Dheevatsa Mudigere, Jorge Nocedal, Mikhail Smelyanskiy, and Ping Tak Peter Tang. On large-batch training for deep learning: Generalization gap and sharp minima, 2016. <http://arxiv.org/abs/1609.04836>.

- [22] Diederik P. Kingma and Jimmy Ba. Adam: A method for stochastic optimization, 2014. <http://arxiv.org/abs/1412.6980>.
- [23] Diederik P. Kingma and Jimmy Ba. Adam: A method for stochastic optimization. In Yoshua Bengio and Yann LeCun, editors, *3rd International Conference on Learning Representations, ICLR 2015, San Diego, CA, USA, May 7-9, 2015, Conference Track Proceedings*, 2015.
- [24] S. Maleki, M. Musuvathi, and T. Mytkowicz. Semantics-preserving parallelization of stochastic gradient descent. In *2018 IEEE International Parallel and Distributed Processing Symposium (IPDPS)*, pages 224–233, 2018.
- [25] Paulius Micikevicius, Sharan Narang, Jonah Alben, Gregory Diamos, Erich Elsen, David Garcia, Boris Ginsburg, Michael Houston, Oleksii Kuchaiev, Ganesh Venkatesh, and Hao Wu. Mixed precision training, 2017. <http://arxiv.org/abs/1710.03740>.
- [26] Boris Polyak and Y.Z. Tsypkin. Pseudogradient adaptation and training algorithms. *Automation and Remote Control*, 34:377–397, 01 1973.
- [27] Alec Radford, Jeff Wu, Rewon Child, David Luan, Dario Amodei, and Ilya Sutskever. Language models are unsupervised multitask learners. 2019.
- [28] Pranav Rajpurkar, Robin Jia, and Percy Liang. Know what you don’t know: Unanswerable questions for squad, 2018. <http://arxiv.org/abs/1806.03822>.
- [29] Pranav Rajpurkar, Jian Zhang, Konstantin Lopyrev, and Percy Liang. Squad: 100,000+ questions for machine comprehension of text, 2016. <http://arxiv.org/abs/1606.05250>.
- [30] Benjamin Recht, Christopher Re, Stephen Wright, and Feng Niu. Hogwild: A lock-free approach to parallelizing stochastic gradient descent. In J. Shawe-Taylor, R. S. Zemel, P. L. Bartlett, F. Pereira, and K. Q. Weinberger, editors, *Advances in Neural Information Processing Systems 24*, pages 693–701. Curran Associates, Inc., 2011.
- [31] David E. Rumelhart, Geoffrey E. Hinton, and Ronald J. Williams. Learning representations by back-propagating errors. *Nature*, 323(6088):533–536, Oct 1986.
- [32] Olga Russakovsky, Jia Deng, Hao Su, Jonathan Krause, Sanjeev Satheesh, Sean Ma, Zhiheng Huang, Andrej Karpathy, Aditya Khosla, Michael Bernstein, Alexander C. Berg, and Li Fei-Fei. ImageNet Large Scale Visual Recognition Challenge. *International Journal of Computer Vision (IJCV)*, 115(3):211–252, 2015.
- [33] Frank Seide, Hao Fu, Jasha Droppo, Gang Li, and Dong Yu. 1-bit stochastic gradient descent and its application to data-parallel distributed training of speech dnns. In Haizhou Li, Helen M. Meng, Bin Ma, Engsiong Chng, and Lei Xie, editors, *INTERSPEECH*, pages 1058–1062. ISCA, 2014.
- [34] Mohammad Shoeybi, Mostofa Patwary, Raul Puri, Patrick LeGresley, Jared Casper, and Bryan Catanzaro. Megatron-lm: Training multi-billion parameter language models using model parallelism, 2019. <http://arxiv.org/abs/1909.08053>.
- [35] R.A. Vandegeijn. On global combine operations. *Journal of Parallel and Distributed Computing*, 22(2):324 – 328, 1994.
- [36] Thijs Vogels, Sai Praneeth Karimireddy, and Martin Jaggi. Powersgd: Practical low-rank gradient compression for distributed optimization. In H. Wallach, H. Larochelle, A. Beygelzimer, F. d’Alché-Buc, E. Fox, and R. Garnett, editors, *Advances in Neural Information Processing Systems 32*, pages 14259–14268. Curran Associates, Inc., 2019.
- [37] Yang You, Igor Gitman, and Boris Ginsburg. Large batch training of convolutional networks. *arXiv preprint arXiv:1708.03888*, 2017.
- [38] Yang You, Jing Li, Sashank Reddi, Jonathan Hseu, Sanjiv Kumar, Srinadh Bhojanapalli, Xiaodan Song, James Demmel, and Cho-Jui Hsieh. Large batch optimization for deep learning: Training bert in 76 minutes. Technical Report UCB/EECS-2019-103, EECS Department, University of California, Berkeley, Jun 2019.
- [39] Shuxin Zheng, Qi Meng, Taifeng Wang, Wei Chen, Nenghai Yu, Zhiming Ma, and Tie-Yan Liu. Asynchronous stochastic gradient descent with delay compensation for distributed deep learning. *CoRR*, abs/1609.08326, 2016.

A Deriving sequential emulation

Suppose $L_1(w)$ and $L_2(w)$ are two loss functions corresponding to two different examples. Starting from model w_0 , sequential SGD, calculates $w_1 = w_0 - \alpha \nabla L_1(w_0)$ followed by $w_2 = w_1 - \alpha \nabla L_2(w_1)$ where α is a properly set learning rate for both iteration. With forward substitution, $w_2 = w_0 - \alpha(\nabla L_1(w_0) + \nabla L_2(w_1))$. Alternatively, $\nabla L_1(w_0)$ and $\nabla L_2(w_0)$ (note that gradients are both at w_0) are computed in parallel and w is updated with $w'_2 = w_0 - \alpha(\nabla L_1(w_0) + \nabla L_2(w_0))$. Clearly w'_2 and w_2 are different because ∇L_2 was computed at a different point.

A.1 Using Taylor Expansion

Adasum uses an estimation for $\nabla L_2(w_1)$ using the Taylor expansion to capture the effect of the first update on the second update. Note that $\nabla L_2(w_1)$ is a convenient notation for the first order derivative of L_2 and can be re-written with $\frac{\partial L_2}{\partial w} \Big|_{w_1}$. Therefore:

$$\begin{aligned} \nabla L_2(w_1) &= \frac{\partial L_2}{\partial w} \Big|_{w_1} = \frac{\partial L_2}{\partial w} \Big|_{w_0+(w_1-w_0)} = \frac{\partial L_2}{\partial w} \Big|_{w_0} \\ &+ \frac{\partial^2 L_2}{(\partial w)^2} \Big|_{w_0} \cdot (w_1 - w_0) + O(\|w_1 - w_0\|^2) \\ &= \frac{\partial L_2}{\partial w} \Big|_{w_0} - \alpha \frac{\partial^2 L_2}{(\partial w)^2} \Big|_{w_0} \cdot \nabla L_1(w_0) \\ &+ \alpha^2 O(\|\nabla L_1(w_0)\|^2) \\ &\approx \nabla L_2(w_0) - \alpha H_2(w_0) \cdot \nabla L_1(w_0) \end{aligned} \quad (6)$$

where the error is $\alpha^2 O(\|\nabla L_1(w_0)\|^2)$ and $H_2(w_0)$ is the Hessian matrix of loss function L_2 . The quadratic relationship between the error in Formula 6 and the learning rate α helps this approximation as in most training practices, learning rate decays with progress in training. However, computing $H_2(w_0)$ requires significant computation powers as the size of this matrix is the number of model parameters squared and with millions of parameters, even storing the matrix is infeasible.

[18] shows that for models with negative log likelihood loss functions (which is the case for all models studied in this paper), the Hessian matrix can be approximated by the outer product of the gradients. By using Equation 6 and this approximation, $\nabla L_2(w_1)$ can be rewritten by:

$$\nabla L_2(w_1) \approx \nabla L_2(w_0) - \alpha \nabla L_2(w_0) \cdot \nabla L_2(w_0)^T \cdot \nabla L_1(w_0) \quad (7)$$

A.2 Choosing optimal learning rate

For this discussion, we assumed that α was properly chosen for the sequential SGD algorithm. We use Taylor expansion for the loss function $L_2(w_0 - \alpha \nabla L_2(w_0))$ and we will take its derivative with respect to α to find the optimal value:

$$\begin{aligned} L_2(w_0 - \alpha \nabla L_2(w_0)) &\approx L_2(w_0) - \alpha \nabla L_2(w_0)^T \cdot L_2(w_0) \\ &+ \frac{\alpha^2}{2} \nabla L_2(w_0)^T \cdot H_2(w_0) \cdot \nabla L_2(w_0) \\ \implies \frac{\partial L_2(w_0 - \alpha \nabla L_2(w_0))}{\partial \alpha} &= -\nabla L_2(w_0)^T \cdot L_2(w_0) \\ &+ \alpha \nabla L_2(w_0)^T \cdot H_2(w_0) \cdot \nabla L_2(w_0) = 0 \\ \implies \alpha \|\nabla L_2(w_0)\|^4 &= \|\nabla L_2(w_0)\|^2 \implies \alpha = \frac{1}{\|\nabla L_2(w_0)\|^2} \end{aligned} \quad (8)$$

where the last line is derived from the approximating for the Hessian matrix. By putting together Equation 8 and 7,

$\nabla L_2(w_1)$ can be approximated by:

$$\nabla L_2(w_1) \approx \nabla L_2(w_0) - \frac{\nabla L_2(w_0) \cdot \nabla L_2(w_0)^T}{\|\nabla L_2(w_0)\|^2} \nabla L_1(w_0) \quad (9)$$

Therefore, to approximate the sequential SGD semantics in a parallel setting, Adasum uses:

$$\begin{aligned} w_2 &= w_0 - \alpha (\nabla L_1(w_0) + \nabla L_2(w_1)) \approx w_0 \\ &- \alpha (\nabla L_1(w_0) + \nabla L_2(w_0) - \frac{\nabla L_2(w_0) \cdot \nabla L_2(w_0)^T}{\|\nabla L_2(w_0)\|^2} \nabla L_1(w_0)) \\ &= w_0 - \alpha (g_1 + g_2 - \frac{g_2 \cdot g_2^T}{\|g_2\|^2} g_1) \end{aligned} \quad (10)$$

where in the last equality, $\nabla L_1(w_0)$ was replaced by g_1 and $\nabla L_2(w_0)$ by g_2 for simplicity (note that the gradients in the last equality are all from w_0). Equation 5 is derived from Equation 10 by rearranging the terms.

A.3 Convergence Proof for Adasum

[26] discusses the requirements for a training algorithm to converge to its optimal answer. Here we will present a simplified version of Theorem 1 and Corollary 1 from [26].

Suppose that there are N training examples for a model with loss functions $L_1(w), \dots, L_N(w)$ where w is the model parameter and w_0 is the initial model. Define $L(w) = \frac{1}{N} \sum_i L_i(w)$. Also assume that w^* is the optimal model where $L(w^*) \leq L(w)$ for all w s. A training algorithm is *pseudogradient* if:

- It is an iterative algorithm where $w_{i+1} = w_i - \alpha_i h_i$ where h_i is a random vector and α_i is a scalar.
- $\forall \epsilon \exists \delta : E(h_i)^T \cdot \nabla L(w) \geq \delta > 0$ where $L(w) \geq L(w^*) + \epsilon$ and w^* is the optimal model.
- $E(\|h_i\|^2) < C$ where C is a constant.
- $\forall i : \alpha_i \geq 0, \sum_i \alpha_i = \inf$, and $\sum_i \alpha_i^2 < \inf$.

The following Theorem is taken from [26].

Theorem A.1. *A pseudogradient training algorithm converges to the optimal model w^* .*

In this section, we assume that the true gradient, ∇L is bounded at any point. As a reminder, $Adasum(g_1, g_2) = (1 - \frac{g_1 \cdot g_1^T}{2 \cdot \|g_1\|^2}) \cdot g_2 + (1 - \frac{g_2 \cdot g_2^T}{2 \cdot \|g_2\|^2}) \cdot g_1$. As discussed in Section 3.4 Adasum operator reduces N gradients in a binary tree manner. We will prove that the final gradient has all necessary requirements of pseudogradient. First, we discuss the inner product of Adasum final vector with $\nabla L(w)$:

Lemma A.2. *Suppose $X = \{x_1, \dots, x_N\}$ is a random variable distribution. For all a and b independently chosen from X , let's define $Y = Adasum(a, b)$. Assume that θ is the angle between $E(X)$ and $E(Y)$. $\cos \theta > 0.942$.*

Proof.

$$\begin{aligned}
E(Y) &= E(\text{Adasum}(a, b)) = E\left(\left(1 - \frac{a \cdot a^T}{2 \cdot \|a\|^2}\right) \cdot b\right. \\
&\quad \left.+ \left(1 - \frac{b \cdot b^T}{2 \cdot \|b\|^2}\right) \cdot a\right) = E(a) + E(b) - E\left(\frac{a \cdot a^T}{2 \cdot \|a\|^2}\right) \cdot E(b) \\
&\quad - E\left(\frac{b \cdot b^T}{2 \cdot \|b\|^2}\right) \cdot E(a) = 2E(X) - E\left(\frac{a \cdot a^T}{\|a\|^2}\right) \cdot E(X)
\end{aligned} \tag{11}$$

where the last equation comes from the independence of a and b . Next we will calculate, η , the angle between $2E(X) - \frac{a \cdot a^T}{\|a\|^2} \cdot E(X)$ for some arbitrary a . First let's denote $E(X)$ with r and assume the angle between r and a is γ . By using the property of inner product, we have:

$$\begin{aligned}
\cos \eta &= \frac{r^T \cdot \left(2r - \frac{a \cdot a^T}{\|a\|^2} \cdot r\right)}{\|r\| \cdot \left\|2r - \frac{a \cdot a^T}{\|a\|^2} \cdot r\right\|} \\
&= \frac{2\|r\|^2 - \|r\|^2 (\cos \gamma)^2}{\|r\| \cdot \sqrt{4\|r\|^2 + \|r\|^2 (\cos \gamma)^2 - 4\|r\|^2 (\cos \gamma)^2}} \\
&= \frac{2 - (\cos \gamma)^2}{\sqrt{4 - 3(\cos \gamma)^2}}
\end{aligned} \tag{12}$$

By taking a derivative of γ from the last equation, we find the minimum value of $\cos \eta$ to be ≈ 0.9428 which concludes that η is at most 0.108π . Since in Formula 11, $E(Y)$ is calculated over an average of all possible a vectors, we can still guarantee that $E(Y)$ and $E(X)$ have at most an angle of 0.108π since we derived this value for the worst case scenario. \square

Lemma A.3. *With same assumptions as in Lemma A.2, $\|E(X)\| \leq \|E(Y)\| \leq 2\|E(X)\|$.*

Proof. As discussed in Lemma A.2, $E(Y) = 2E(X) - E\left(\frac{a \cdot a^T}{\|a\|^2}\right) \cdot E(X) = (2I - E\left(\frac{a \cdot a^T}{\|a\|^2}\right)) \cdot E(X)$. It is trivial to check that the matrix $(2I - E\left(\frac{a \cdot a^T}{\|a\|^2}\right))$ is symmetric with eigenvalues between 1 and 2. Therefore, $\lambda_{\min} \|X\| \leq \|Y\| \leq \lambda_{\max} \|X\|$ where λ_{\min} and λ_{\max} are respectively the smallest and largest eigenvalues of the aforementioned matrix. \square

Assumption: Lemma A.2 showed that in the worst case $E(Y)$ can rotate at most 0.108π with respect to $E(X)$. Even meeting this worst case requires carefully crafted x_i s. If Adasum was applied recursively on X ($Y = \text{Adasum}(X, X), Z = \text{Adasum}(Y, Y), \dots$) for k times, the expected value of final distribution will at most have an angle of $0.108k\pi$ which is only possible if each Adasum meets the worst case scenario and each worst case is stacked over the previous one. As one can imagine, this is an extremely unlikely scenario. In case x_i s are gradients, we assume that Adasum recursively always keeps the angle with $E(X)$ to at most σ where $\cos \sigma > 0$. Using

this assumption and Lemma A.3, we can prove that Adasum algorithm is a pseudogradient training algorithm.

Theorem A.4. *Adasum algorithm applied in an iterative manner using a proper learning rate on a set of N gradients, $G = \{g_1, \dots, g_N\}$ computed in parallel, is a pseudogradient training algorithm.*

Proof. Given that Adasum follows the iterative method of SGD, the first assumption of a pseudogradient training algorithm is met. Also, since we use the learning rate schedule from the converging sequential SGD, the requirement for the learning rate is trivially met. Section 3.4 discussed how Adasum reduces all gradients in a binary tree manner which has $\log N$ steps. The distribution of the leaf level in this binary tree is G and the next level's distribution is $G_1 = \text{Adasum}(G, G)$. Level i 's distribution is $G_{i+1} = \text{Adasum}(G_i, G_i)$. At the top of the tree, we have $G_{\log N}$ as the distribution. Using Lemma A.3, $\|E(G)\| \leq \|E(G_{\log N})\| \leq 2^{\log N} \|E(G)\| = N \|E(G)\|$. Since $E(G)$ is the true gradient ($\nabla L(w_i)$), $\|E(G)\|$ is bounded by assumption and therefore, so is $\|E(G_{\log N})\|$. This meets the requirement for the norm of the h_i s. Finally, Lemma A.3 proves that $E(G) \leq \|E(G_{\log N})\|$ and therefore $E(G_{\log N})^T E(G) \geq \|E(G_{\log N})\| \|E(G)\| \cos \sigma \geq \|E(G)\|^2 \cos \sigma$. For any w_i which is not w^* , $\|E(G)\| > 0$ and based on the assumption, $\cos \sigma > 0$. Therefore, the positive inner product assumption is also met which concludes that Adasum is a pseudogradient training algorithm and it converges. \square

A.4 Adasum Convergence Rate

Convergence rate of Adasum is highly dependent on orthogonality of the gradients. In the worst case scenario if all gradients are parallel, the algorithm converges in $1/N$ rate of the sequential SGD where N is the number of processors and in the best case where all of the gradients are orthogonal, we expect Adasum to converge as fast as the sequential SGD.

A.5 Convergence of Adasum with Learning Rate Optimizers

The kernel of the computation in all optimizers such as Adam, LAMB or LARS is computing the gradients. These optimizers differ by having different learning rate mechanisms for each parameter. Generally one can think of having a dynamic learning rate per layer for each of these optimizers. At each iteration i and for each layer l , let's define $\Delta_i^l = w_{i+1}^l - w_i^l$ to be the update term for layer l . If g_i^l is the corresponding gradient at iteration i , $\Delta_i^l \approx C_i^l \cdot g_i^l$ where C_i^l is a scalar. This approximation is true in expectation for all optimizers that use an unbiased gradient.

Adasum reduces all Δ_i^l across all GPUs for each layer and since Δ_i^l is approximately a constant multiplied by the gradi-

ent, Adasum applied on Δ_i^l s is the same as applying it on g_i^l scaled by the same constant.